Available on CMS information server **CMS CR 2006/056**

CMS Conference Report

8 September 2006

Search for Z-primes and Randall-Sundrum Gravitons with dimuons in CMS

P. Traczyk

Soltan Institute for Nuclear Studies, Warsaw, Poland

for the CMS collaboration

Presented at "Physics at LHC" July 2006 Kraków, Poland

Abstract

This paper presents results from studies on observability of Z' particles and Randall-Sundrum gravitons in the dimuon channel in the CMS detector. Full detector simulation and reconstruction were carried out to derive both the discovery potential and results for model discrimination. Effects of systematic uncertainties on the expected reach of the CMS experiment are also presented.

1 Introduction

A new heavy neutral boson decaying into lepton pairs can provide a striking signal of new physics at the LHC. Two types of particles giving such signature are currently considered - a spin-2 graviton excitation and a spin-1 extra gauge boson (Z').

Z' is a generic name for new neutral gauge bosons appearing in many models, including models of dynamical symmetry breaking [1], little Higgs [2] models, also superstring-inspired [3] and grand unified theories [4]. Excited gravitons appear in models with extra dimensions, in particular a narrow Z'-like resonance is predicted by the Randall-Sundrum (RS) [5] model.

The couplings of the Z' are fixed by the choice of the theoretical framework, and the only free parameter is its mass. Experimental lower limits on this mass are of the order of 600-900 GeV [6], while theory currently does not provide any reliable predictions.

The phenomenology of the Randall-Sundrum model is governed by two parameters. The first is the mass of the first graviton excitation, and the second is $c = k/M_{Pl}$ determining the couplings and width of the graviton. Experimental and theoretical bounds on these parameters form a closed allowed region in parameter space, with masses up to 4 TeV, and k/M_{Pl} between 0.01 and 0.1 [7].

2 Signal and background processes

Signal and background samples were generated with PYTHIA [8] 6.227 (with the CTEQ6L set of parton distribution functions [9]) and processed through full CMS detector simulation and reconstruction software.

RS gravitons were simulated with mass values of 1, 1.5, 2, 3 and 4 TeV, and values of $k/M_{Pl} = 0.01, 0.02, 0.05, 0.10$. Z' particles vere simulated with masses of 1,3 and 5 TeV, with six different sets of couplings corresponding to six different models predicting an extra neutral gauge boson: $Z_{\rm SSM}$, the Sequential Standard Model (SSM) Z', with couplings the same as the Standard Model Z^0; Z_ψ, Z_η and Z_χ, arising in E_6 and SO(10) GUT groups; $Z_{\rm LRM}$ and $Z_{\rm ALRM}$, appearing in the so-called "left-right" and "alternative left-right" models. Further details on the various types of Z' and their couplings are given in Ref. [10].

The Standard Model (SM) background for the processes under study consistis mainly of Drell-Yan dimuon production. Other possible sources of high energy muon pairs ($t\bar{t}$, $b\bar{b}$ and Z and W boson pair production) have been found to have a contribution an order of magnitude lower than Drell-Yan, and can be further suppressed by requiring that the reconstructed muons be isolated. Hence, only Drell-Yan was considered in this work.

3 Search for a resonance

Signal observability was estimated by performing maximum-likelihood fits to reconstructed dimuon invariant mass spectra and calculating the value of the significance estimator $S_L = \sqrt{2\ln(\mathcal{L}_{s+b}/\mathcal{L}_b)}$, where $\mathcal{L}_b$ and $\mathcal{L}_{s+b}$ are the best-fit likelihoods of the pdf's corresponding to the null hypothesis H_0 (no signal present) and the alternative hypothesis H_1 (signal plus background), respectively. The relative normalization of the signal and background processes is a free parameter of the fit - the analysis exploits the difference in shape between the signal (a quasi-gaussian peak) and the background (an exponentially falling continuum). A more in-depth look at this and other methods of estimating discovery significance is given in Refs [12] and [10].

3.1 Treatment of systematic uncertainties

There are two types of sources of systematic uncertainty in this analysis. The first are theoretical uncertainties on the signal and background cross-sections, due mainly to parton distribution function (pdf), hard process scale uncertainties and higher order QCD and electroweak corrections. Since the analysis does not rely on any assumptions about signal and background normalization, these uncertainties affect only the reach estimate, and will not have any direct impact on significance calculation based on real data. These uncertainties were combined in quadrature, and translated into 1σ uncertainty in the predicted discovery reach.

The second type of systematic uncertainties are uncertainties resulting from imperfect knowledge of the experimental condidions. These include pileup, tracker and muon system misalignment, magnetic field and muon detector calibration uncertainty. In this study, misalignment and pileup were taken into account during detector simulation, while other effects were found to be negligible.

The results for CMS 5σ discovery reach are shown in Figs 1 and 2.

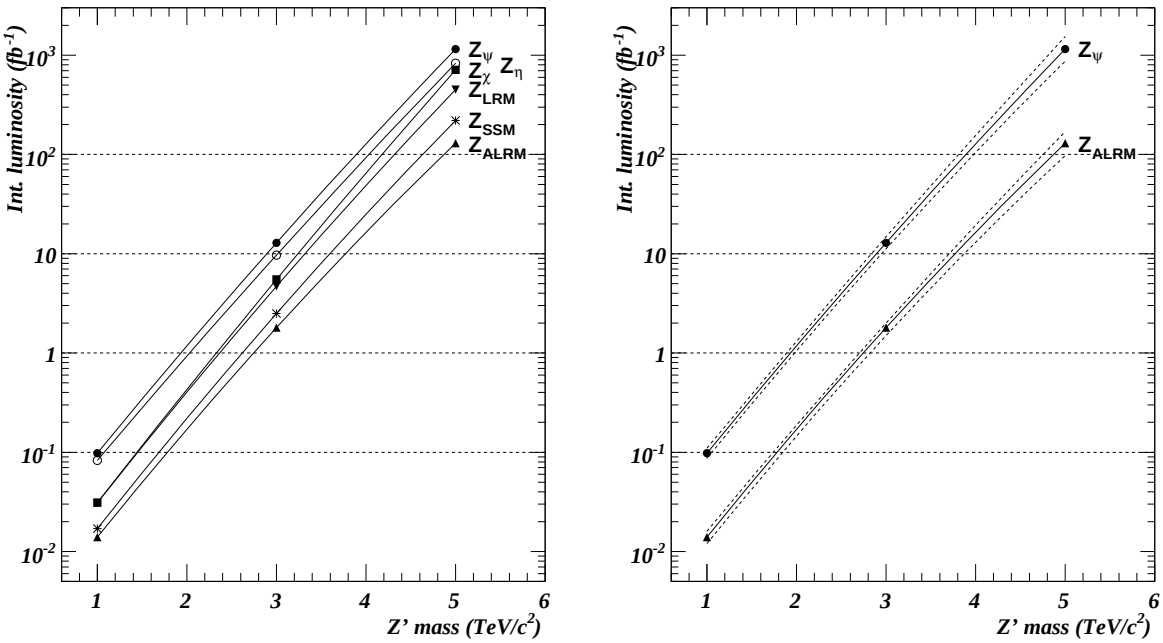

Figure 1: Integrated luminosity needed to reach 5σ significance as a function of Z$'$ mass. The left plot shows results with statistical uncertainties only, the right plot shows results with systematics, for two of the considered models. Solid lines show the best estimates, dashed lines correspond to $\pm 1\sigma$ theoretical uncertainty.

4 Model discrimination

After a new resonance has been discovered, its identity has to be established by measuring its various properties. A graviton can be distinguished from a Z$'$ because of it's spin-2 nature. Different Z$'$ particles originating from different models can be distinguished by measuring the forward-backward asymmetry ($A_{\rm FB}$) of the final state muons.

4.1 Spin discrimination

The spin of the observed resonance manifests itself in the angular distributions of its decay products:

subprocess	angular distribution
$q\bar{q} \to \gamma/Z^0/Z' \to f\bar{f}$	$\frac{3}{8}(1+\cos\theta^{*2})$
$q\bar{q} \to G^* \to f\bar{f}$	$\frac{5}{8}(1-3\cos\theta^{*2}+4\cos\theta^{*4})$
$gg \to G^* \to f\bar{f}$	$\frac{5}{8}(1-\cos\theta^{*4})$

where $\cos\theta^*$ is the angle between the incident quark or gluon and the outgoing lepton. In an experimental situation the transverse momenta of the incoming partons are not known, and optimal results are achieved by calculating $\cos\theta^*$ in the Collins-Soper frame [13]. In order to reduce the contamination from the Drell-Yan background, only events in a $\sim 2\sigma$ mass window around the resonance peak were used in the analysis.

The analysis closely follows the method described in Ref. [11], where an unbinned likelihood is calculated for the graviton and Z', under the two hypotheses considered. The test statistic used to distinguish the two hypotheses is the likelihood ratio: $-2\ln\lambda = 2\ln\mathcal{L}_1 - 2\ln\mathcal{L}_2$.

The test was constructed to treat the two hypotheses equally, ie. with equal probabilities of Type-I and Type-II errors. The CMS reach for 2σ discrimination in the M_G-k/M_{Pl} plane for different values of integrated luminosity is shown in Fig. 3

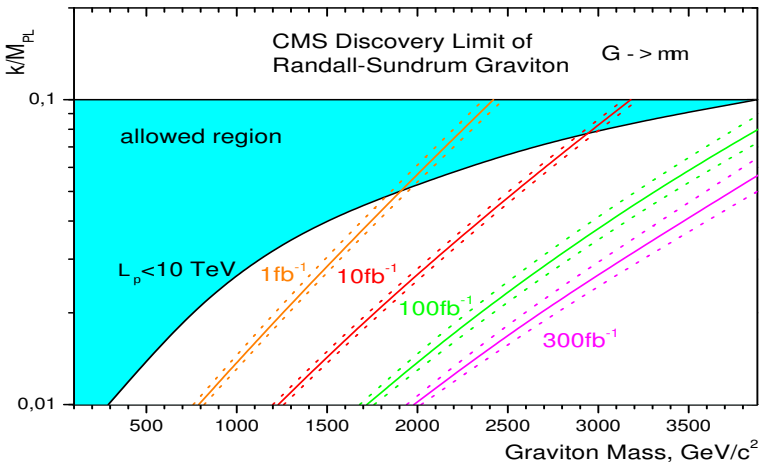

Figure 2: Theoretical and experimental constraints on the RS model parameters, with systematic uncertainties taken into account. The region to the left of the curves corresponds to 5σ discovery reach, for different values of integrated luminosity.

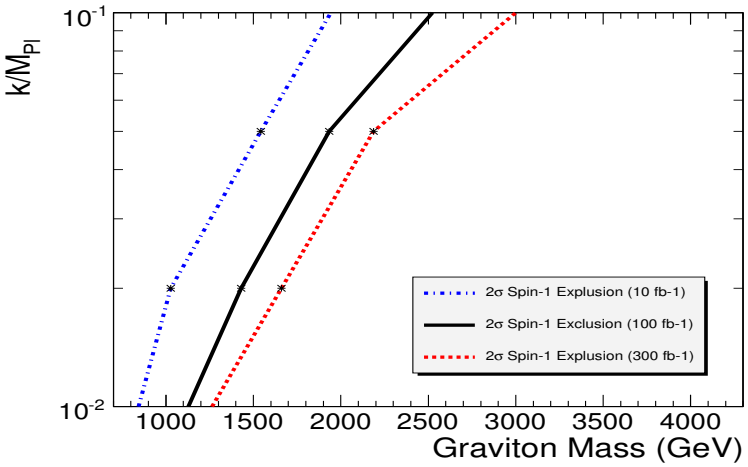

Figure 3: CMS reach for 2σ discrimination between spin-1 and spin-2 hypotheses in the Randall-Sundrum model parameter space, for different values of integrated luminosity. The accessible region lies to the left of the curves.

4.2 A_{FB} measurement

In the $q\overline{q} \to \gamma/\mathrm{Z}^0 \to \ell^+\ell^-$ channel, A_{FB} arises from the combination of parity-conserving couplings (from the γ) and parity-violating couplings (from the Z^0) in the interaction Lagrangian. A Z' contributes another parity-violating term, shifting the value of A_{FB}, especially in the mass range around the peak, as shown in Fig. 4.

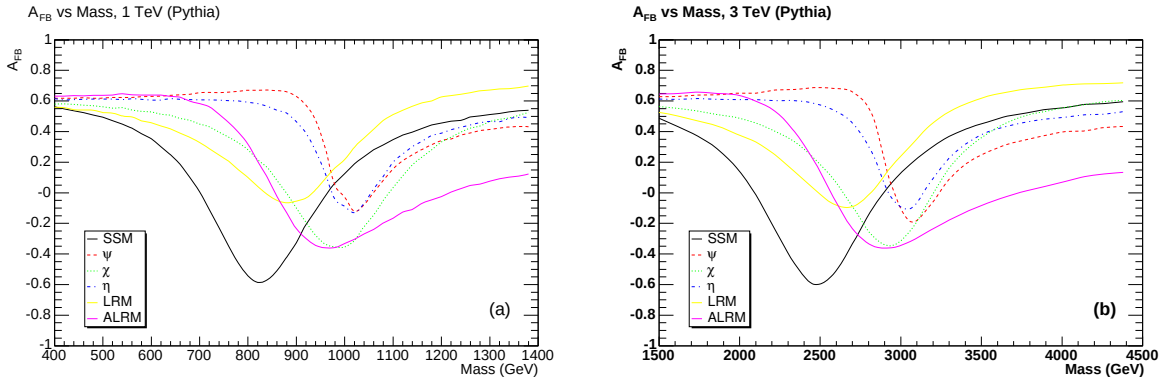

Figure 4: A_{FB} vs $M_{\mu\mu}$ for $pp \to \gamma/\mathrm{Z}^0/\mathrm{Z}' \to \mu^+\mu^-$ generated events with Z' mass set to (a) 1 TeV and (b) 3 TeV.

As opposed to the spin discrimination case, for A_{FB} measurement the terms odd in $\cos\theta^*$ are important. Since the angle θ is measured with respect to the direction of the incoming quark, the study of A_{FB} in proton-proton interactions is troublesome. This is due to the fact that a quark can originate with equal probability from either proton, and the sign of $\cos\theta^*$ is not directly measurable. Here it is assumed that the longitudinal motion of the dimuon system is in the direction of the proton contributing the annihilating quark, since a quark in a proton typically carries a larger momentum fraction x than does an antiquark. This introduces an uncertainty in the asymmetry measurement.

The value of A_{FB} is extracted from data by performing a multi-dimensional maximum likelihood fit, taking into account the probability of incorrect assignment of the sign of $\cos\theta^*$, the detector acceptance, and resolution. The rapid variation of A_{FB} with $M_{\mu\mu}$ shown in Fig. 4 will be hard to observe with real data, due to limited statistics and mass resolution. In this work only the mass peak region is considered, to investigate to what extent different models can be distinguished.

Fig. 5 contains a graphical representation of the results. The vertical axis is split into six regions, one for each of the six models studied. On the horizontal axis, the value A_{FB} for each model is represented by an asterisk and a vertical dotted line spanning the plot; a triangle marker with error bars indicates the expected error on $A_{\mathrm{FB}}^{\mathrm{rec}}$ with 10 fb^{-1} (for a 1 TeV Z' mass shown in (a)) or 400 fb^{-1} (for a 3 TeV Z' mass shown in (b)) of integrated luminosity. Solid vertical lines are drawn halfway between the adjacent values of A_{FB}, forming the boundaries of the critical regions, $A_{\mathrm{FB}}^{\mathrm{cut}}$, for the respective pairs of models.

Table 1 gives a summary of the values of the significance level for pairwise comparisons of Z' models at $M_{\mathrm{Z}'} = 1$ TeV and with 10 fb^{-1} of integrated luminosity. The left column specifies the model taken as the null hypothesis H_0, which is tested against the alternative of each of the other five models in the adjacent columns.

Model	$\mathrm{Z}_{\mathrm{ALRM}}$	Z_{χ}	Z_{η}	Z_{ψ}	$\mathrm{Z}_{\mathrm{SSM}}$	$\mathrm{Z}_{\mathrm{LRM}}$
$\mathrm{Z}_{\mathrm{ALRM}}$	–	0.0	5.3	6.6	7.6	9.4
Z_{χ}	0.0	–	3.7	4.6	5.3	6.6
Z_{η}	2.7	2.6	–	0.7	1.2	2.1
Z_{ψ}	3.3	3.3	0.7	–	0.5	1.4
$\mathrm{Z}_{\mathrm{SSM}}$	6.8	6.8	2.1	0.9	–	1.6
$\mathrm{Z}_{\mathrm{LRM}}$	6.8	6.8	3.0	2.1	1.3	–

Table 1: Significance level α (expressed in equivalent number of σ's) for pairwise comparisons of Z' models at $M_{\mathrm{Z}'} = 1$ TeV, for 10 fb^{-1} of integrated luminosity.

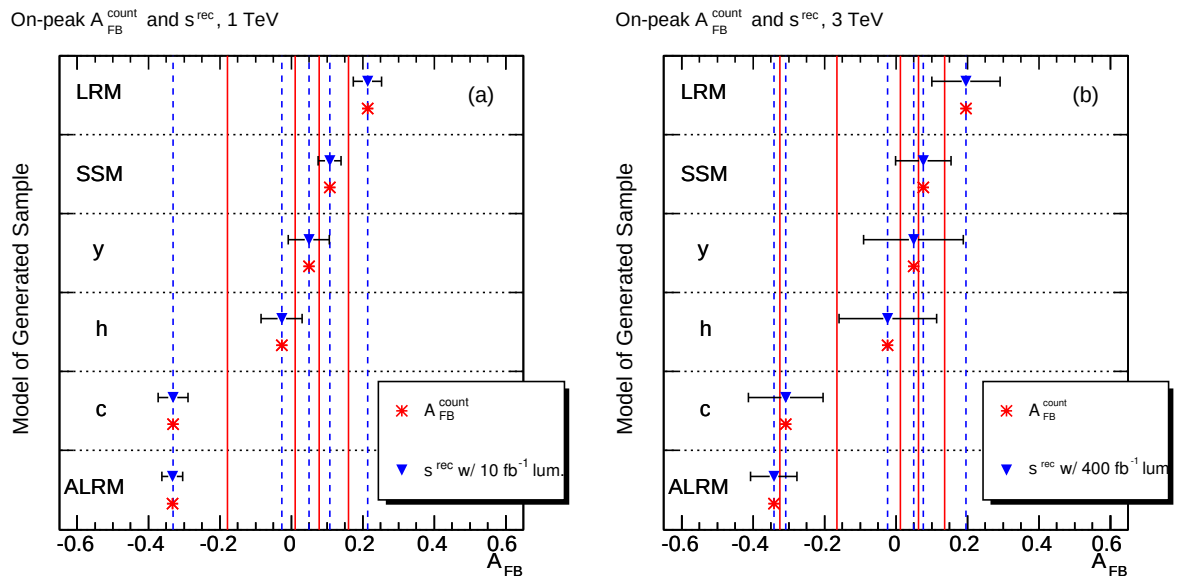

Figure 5: On-peak $A_{\rm FB}$ with expected statistic alerrors, for (a) $M_{\rm Z'} = 1$ TeV and (b) $M_{\rm Z'} = 3$ TeV. The dotted vertical lines and asterisks show the $A_{\rm FB}$ for each model. The solid vertical lines are halfway between the adjacent $A_{\rm FB}$. The error bars on the triangle markers correspond to (a) 10 fb^{-1} and (b) 400 fb^{-1} of integrated luminosity.

5 Conclusions

The above results show that high energy muon pairs provide a promising signature for searches for new heavy bosons. Even with an integrated luminosity of only 0.1-1 fb^{-1} and non-optimal alignment a 5σ disovery is possible for particles with mass of 1-2 TeV. For a luminosity of 100 fb^{-1} and optimal alignment, the discovery reach is in the range between 3.9 and 4.8 TeV for a Z$'$ and 1.7 to 4.1 TeV for a RS graviton.

Spin-1 and spin-2 hypotheses can be discriminated at 2σ level for gravitons with mass up to 1.1 TeV for $c = 0.01$ and 2.5 TeV for $c = 0.1$, with an integrated luminosity of $\int Ldt$ = 100 fb^{-1}. With 400 fb^{-1} of data, the measurement of forward-backward asymmetry can be used to distinguish between either $\rm Z_{ALRM}$ or $\rm Z_\chi$ and one of the other four studied models ($\rm Z_{SSM}$, $\rm Z_\psi$, $\rm Z_\eta$, or $\rm Z_{LRM}$) up to a $M_{\rm Z'}$ between 2.0 and 2.7 TeV. The $\rm Z_{SSM}$, $\rm Z_\psi$, $\rm Z_\eta$, and $\rm Z_{LRM}$ are distinguishable with the same level of significance only up to $M_{\rm Z'} = 1$–1.5 TeV, and $\rm Z_{ALRM}$ and $\rm Z_\chi$ are indistinguishable for masses over 1 TeV.

Furter details of the analyses presented in this paper can be found in the corresponding CMS Notes [14, 15, 16]. This work was partially financed by Polish Ministry of Science in 2006-2007 as a research project.

References

[1] For a review, see C.T. Hill and E.H. Simmons, "Strong Dynamics and Electroweak Symmetry Breaking", Phys. Rep. **381** (2003) 235.

[2] See, for example, T. Han et al., "Phenomenology of the Little Higgs Model", Phys. Rev. **D 67** (2003) 095004.

[3] M. Cvetič and P. Langacker, "Implications of Abelian Extended Gauge Structures From String Models", Phys. Rev. **D 54** (1996) 3570; "New Gauge Bosons From String Models", Mod. Phys. Lett. **A 11** (1996) 1247.

[4] For a review, see A. Leike, "The Phenomenology of Extra Neutral Gauge Bosons", Phys. Rep. **317** (1999) 143.

[5] L. Randall and R. Sundrum, "A large mass hierarchy from a small extra dimension", *Phys. Rev. Lett.* **83** (1999) 3370; "An alternative to compactification", *Phys. Rev. Lett.* **83** (1999) 4690.

[6] Review of Particle Properties, K. Hagiwara et al., Phys. Rev. **D 66** (2002) 328,
The LEP Collaborations, the LEP Electroweak Working Group, the SLD Electroweak and Heavy Flavour Groups, "A Combination of Preliminary Electroweak Measurements and Constraints on the Standard Model", CERN-PH-EP/2004-069, hep-ex/0412015.

[7] H. Davoudiasl, J.L. Hewett and T.G. Rizzo, "Experimental Probes of Localized Gravity: On and Off the Wall", *Phys. Rev.* **D63** (2001) 075004.

[8] T. Sjöstrand et al., "High-Energy-Physics Event Generation with PYTHIA 6.1", Comput. Phys. Commun. **135** (2001) 238.

[9] J. Pumplin et al., "New Generation of Parton Distributions with Uncertainties from Global QCD Analysis", JHEP **07** (2002) 012.

[10] R. Cousins, J. Mumford, V. Valuev, "Detection of Z' Gauge Bosons in the Dimuon Decay Mode in CMS", CMS Note 2005/002.

[11] R. Cousins et al., "Spin Discrimination of New Heavy Resonances at the LHC", JHEP **11** (2005) 046.

[12] V. Bartsch and G. Quast, "Expected Signal Observability at Future Experiments", IEKP-KA/2003-30, CMS Note 2005/004.

[13] J. Collins and D. Soper, "Angular Distribution of Dileptons in High-Energy Hadron Collisions", *Phys. Rev.* **D 16** (1977) 2219.

[14] R. Cousins, J. Mumford and V. Valuev, "Detection of Z' Gauge Bosons in the Dimuon Decay Mode in CMS", CMS Note 2006/062.

[15] R. Cousins, J. Mumford, V. Valuev, "Forward-Backward Asymmetry of Simulated and Reconstructed $\mathrm{Z}' \to \mu^+\mu^-$ Events in CMS", CMS Note 2005/022.

[16] I.Belotelov et al., "Search for Randall-Sundrum Graviton Decay into Muon Pairs", CMS Note 2006/104.